An Initial Approach to Biologically Related Bridged Assemblies: Pyridinethiolate-Linked Fe_4S_4–Fe Complex Systems

Hong Ye Liu, Bernd Scharbert,[1] and R. H. Holm*

Contribution from the Department of Chemistry, Harvard University, Cambridge, Massachusetts 02138. *Received April 29, 1991*

Abstract: The subsite-differentiated cubane-type clusters $[Fe_4S_4(LS_3)L']^{z-}$ (LS_3 = 1,3,5-tris((4,6-dimethyl-3-mercaptophenyl)thio)-2,4,6-tris(*p*-tolylthio)benzene(3−)) undergo substitution reactions at the unique subsite. This property has been exploited in the formation of bridged assemblies in which an Fe_4S_4 cluster and a high-spin Fe(II) complex are covalently linked. Reaction of $[Fe_4S_4(LS_3)(SR)]^{2-}$ (R = Me, Et) with isomeric pyridinethiols (HSpy) affords $[Fe_4S_4(LS_3)(S\text{-}2\text{-}py)]^{2-}$ (**7**), $[Fe_4S_4(LS_3)(S\text{-}3\text{-}py)]^{2-}$ (**8**), and $[Fe_4S_4(LS_3)(S\text{-}4\text{-}py)]^{2-}$ (**9**). Cluster **7** did not react with Fe(acen) (acen = *N,N'*-ethylenebis(acetylacetoneiminate(2−)) because of the chelate structure at the unique subsite. Reaction of **8** with Fe(acen) gives **8**-Fe(acen), and reaction of **9** with Fe(acen) and Fe(tfacen) (tfacen = *N,N'*-bis(trifluoroacetylacetoneiminate(2−)) forms **9**-Fe(acen) and **9**-Fe(tfacen). Bridge formation was readily detected from the isotropically shifted ^1H NMR spectra, which are fast-exchange averages over the bridged species and their separate components. An NMR method was developed for determination of formation constants of pyridine adducts in the systems Fe(acen)/py and Fe(tfacen)/py and in those containing the bridged species. For **9**-Fe(acen) and **9**-Fe(tfacen), K_f = 790 and 920 M^{-1}, respectively, in acetonitrile solution. Bridge-Fe(II) binding is expected to resemble that in $Fe(tfacen)(py)_2$, whose structure (trans octahedral) is reported. Bridge formation was also detected electrochemically; in the case of Fe(acen) a reversible oxidation reaction occurs only when the complex is axially ligated by a pyridyl ligand. The effects of ligand substituents on equilibrium constants and redox potentials are described. The preparative and redox reactions generate the bridged assembly oxidation levels $[Fe_4S_4]^{1+}$/[Fe(II)], $[Fe_4S_4]^{2+}$/Fe(II), and $[Fe_4S_4]^{2+}$/Fe(III), which are those known for the bridged Fe_4S_4–siroheme active site assembly of *E. coli* sulfite reductase. This work provides the initial experimental protocol for the construction of biologically related, bridged Fe_4S_4–Fe complex assemblies that should allow examination of such matters as electron transfer and magnetic coupling between cluster and Fe(II,III) sites. Potential means for forming nonlabile bridged assemblies are outlined, including the covalent attachment of an iron complex to the bridging group with use of a five-coordinate ligand. The preparation and structure of one such complex, *N,N'*-2,6-diethylpyridinebis(trifluoroacetyliminato)iron(II), are described.

Introduction

Native Fe_4S_4 clusters in certain proteins and enzymes exhibit what we have termed "subsite-specific properties".[2] These are structural and reactivity features that are localized at a specific iron subsite, which is differentiated from the other three cysteinate-bound subsites by the identity of its terminal ligand(s). Such properties have been considered at some length elsewhere.[2] The cubane-type clusters $[Fe_4S_4(LS_3)L']^z$ (**1**) have been shown to be effective synthetic analogues[3,4] for native Fe_4S_4 clusters whose

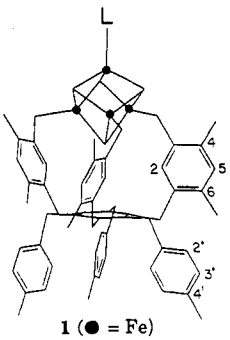

1 (● = Fe)

2: L' = Cl^-

3: L' = RS^-

subsites are differentiated in a 3:1 ratio. Subsite differentiation is effected by the semirigid trithiolate ligand LS_3,[5] which disposes three coordinating "arms" above and three buttressing "legs" below, the central benzene ring. A detailed conformational analysis of cluster **1** has been carried out.[4] The indicated trigonal symmetry of **1** is consistent with the ^1H NMR spectra of over 30 clusters examined in this laboratory[2-4,6-9] and has been crystallographically demonstrated in the Ph_4P^+ salt of $[Fe_4Se_4(LS_3)Cl]^{2-}$.[4] Chloride cluster **2** supports a wide variety of subsite-specific substitution reactions, involving mono- and polydentate ligands.[6-9] Alkylthiolate cluster **3** is also a useful precursor inasmuch as it undergoes clean substitution reactions with arylthiols at the unique subsite.[3]

Among the enzymes manifesting site-specific properties are aconitase and the assimilatory sulfite reductase from *Escherichia coli* (*Ec* SiR), both of which have been crystallographically examined. Aconitase binds water or hydroxide at the unique subsite.[10,11] *Ec* SiR, which catalyzes the reduction of sulfite to sulfide, contains a covalently bridged, magnetically coupled cluster-siroheme assembly.[12-15] The active site structure[14] from X-ray

(1) Postdoctoral Fellow of the Deutsche Forschungsgemeinschaft, 1988-1989.
(2) Holm, R. H.; Ciurli, S.; Weigel, J. A. *Prog. Inorg. Chem.* **1990**, *38*, 1.
(3) Stack, T. D. P.; Holm, R. H. *J. Am. Chem. Soc.* **1988**, *110*, 2484.
(4) Stack, T. D. P.; Weigel, J. A.; Holm, R. H. *Inorg. Chem.* **1990**, *29*, 3745.
(5) LS_3 = 1,3,5-tris((4,6-dimethyl-3-mercaptophenyl)thio)-2,4,6-tris(*p*-tolylthio)benzene(3−).
(6) Stack, T. D. P.; Carney, M. J.; Holm, R. H. *J. Am. Chem. Soc.* **1989**, *111*, 1670.
(7) Ciurli, S.; Carrie, M.; Weigel, J. A.; Carney, M. J.; Stack, T. D. P.; Papaefthymiou, G. C.; Holm, R. H. *J. Am. Chem. Soc.* **1990**, *112*, 2654.
(8) Weigel, J. A.; Srivastava, K. K. P.; Day, E. P.; Münck, E.; Holm, R. H. *J. Am. Chem. Soc.* **1990**, *112*, 8015.
(9) Weigel, J. A.; Holm, R. H. *J. Am. Chem. Soc.* **1991**, *113*, 4184.
(10) Robbins, A. H.; Stout, C. D. *Proc. Natl. Acad. Sci. U.S.A.* **1989**, *86*, 3639. *Proteins* **1989**, *5*, 289.
(11) Werst, M. M.; Kennedy, M. C.; Beinert, H.; Hoffman, B. M. *Biochemistry* **1990**, *29*, 10526.
(12) (a) Janick, P. A.; Siegel, L. M. *Biochemistry* **1982**, *21*, 3538; **1983**, *22*, 504. (b) Chrisiner, J. A.; Münck, E.; Janick, P. A.; Siegel, L. M. *J. Biol. Chem.* **1983**, *256*, 11147. (c) Christner, J. A.; Janick, P. A.; Siegel, L. M.; Münck, E. *J. Biol. Chem.* **1983**, *258*, 11157. (d) Christner, J. A.; Münck, E.; Kent, T. A.; Janick, P. A.; Salerno, J. C.; Siegel, L. M. *J. Am. Chem. Soc.* **1984**, *106*, 6786. (e) Cline, J. F.; Janick, P. A.; Siegel, L. M.; Hoffman, B. M. *Biochemistry* **1986**, *25*, 4647.
(13) Madden, J. F.; Han, S.; Siegel, L. M.; Spiro, T. G. *Biochemistry* **1989**, *28*, 5471.
(14) McRee, D. D.; Richardson, D. C.; Richardson, J. S.; Siegel, L. M. *J. Biol. Chem.* **1986**, *261*, 10277.
(15) Ostrowski, J.; Wu, J.-Y.; Rueger, D. C.; Miller, B. E.; Siegel, L. M.; Kredich, N. M. *J. Biol. Chem.* **1989**, *264*, 15726. This article contains a space-filling model of the catalytic site.

0002-7863/91/1513-9529$02.50/0

analysis is depicted schematically as **4**, with a 4.4 Å separation

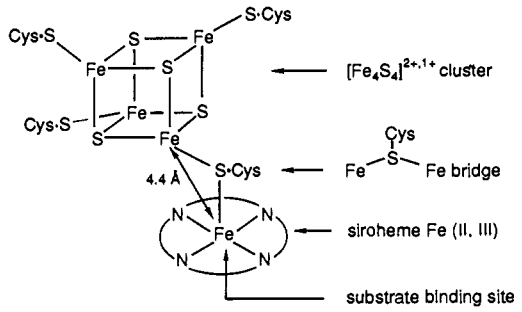

4

between the siroheme iron atom and the nearest iron atom in the cluster. The bridging ligand is probably a cysteinyl sulfur atom, but this cannot be considered as proven from the X-ray data. The assimilatory sulfide reductase from *Desulfovibrio vulgaris* (*Dv* SiR) has been proposed to contain an exchange-coupled Fe_4S_4 cluster and a siroheme group, possibly bridged by sulfide.[16,17] This view has recently been challenged on the basis of a study of a dissimilatory *Dv* SiR.[18] No X-ray structural data are available for these enzymes.

A simple, attractive picture of substrate reduction by *Ec* SiR involves substrate binding at the vacant axial site of siroheme, with coupled steps of electron transfer from cluster to substrate and protonation until sulfide is formed. The electron-transfer pathway may involve the bridge or possibly proceed from cluster to siroheme directly inasmuch as, from electron density maps, the two appear to be within van der Waals contact in *Ec* SiR.[14]

The unique assembly **4**, which provides the most intimate juxtaposition of an electron transfer and a catalytic prosthetic group yet unknown in any metalloenzyme, raises a number of questions. Considering the putative Fe–(S-Cys)–Fe and Fe–S–Fe bridges, do they owe their stability to the protein structure? Equivalently, is such a bridged assembly capable of independent existence? The pathway of electron transfer from cluster to substrate—direct from cluster to macrocycle or through a bridge—is unknown. Similarly obscure is the natural selection of siroheme itself, whose sirohydrochlorin macrocycle is at the isobacteriochlorin oxidation level. Are the properties of ready oxidation, conformational flexibility, and hole size of the macrocycle all considered relative to a porphyrin, critical factors in enzyme action?[19] Lastly, can a synthetic sulfite reductase system be constructed based on a bridged assembly? These matters also pertain to nitrite reductase, which, based on spectroscopic results, has the same active site assembly as SiR or a coupled assembly of cluster and siroheme very similar to it.[20]

We consider it probable that at least some of the foregoing points can be addressed profitably in synthetic systems, where control can be exercised on certain potential structural variables such as the type of bridge, the separation of cluster and iron complex, and the nature of the iron macrocyclic complex. However, a deliberate approach to the desired assemblies was unavailable prior to the synthesis of the subsite-differentiated clusters **1**. Here we show that Fe_4S_4–Fe complex bridged assemblies can be prepared by a subsite-specific procedure that should ultimately allow considerable variation in bridge structure and iron complex. The present systems are not necessarily intended as models for a native assembly. Rather, they illustrate an approach that we intend to elaborate in order to examine the effects of structural variables on bridged assemblies and their ability to execute substrate reduction. Only recently have bridging interactions involving Fe_4S_4 clusters been demonstrated. These take the form of linkage between two clusters by means of a dithiolato, oxo, sulfido, or selenido bridge. Except for $[(Fe_4S_4Cl_3)_2S]^{4-}$,[21] these double-cubanes were prepared by subsite-specific reactions of cluster **2**.[6,9]

Experimental Section

Preparation of Compounds. All operations were performed under a pure dinitrogen atmosphere using standard Schlenk techniques or an inert atmosphere box. Solvents were dried and degassed prior to use. The cluster compounds below were not analyzed because of the small scale of most of the preparations. As in previous work,[3,4,6-9] the full or substantial purity of the compounds was established by their ^1H NMR spectra, which were recorded in CD_3CN solutions. NMR signal assignments correspond to the numbering scheme of **1**. Cluster compounds of this type were isolated after solvent removal as dark brown or black, air-sensitive solids that are soluble in acetonitrile, dichloromethane, and THF. Yields refer to weighed amounts of solids removed from reaction flasks; in situ yields are essentially quantitative.

Clusters. (a) $(Bu_4N)_2[Fe_4S_4(LS_3)(SMe)]$ ($(Bu_4N)_2$**[5]**). To a solution of 500 mg (0.49 mmol) of $(Bu_4N)_2[Fe_4S_4(SMe)_4]$[22] in 50 mL of acetonitrile was added a slurry of 500 mg (0.53 mmol) of $L(SH)_3$[4] in 50 mL of chloroform. The reaction mixture was stirred under dynamic vacuum for 6 h, and then the solvent was evaporated. The solid residue was dissolved in acetonitrile, and the solution was filtered. The ^1H NMR spectrum of the solid obtained from a small aliquot of the filtrate showed the major product to be the desired compound but with about 20% of $(Bu_4N)_2$**[2]** (formed from chloroform or a chloride-containing impurity). Solid NaSMe (16.9 mg, 0.24 mmol) was added to the acetonitrile solution, and the mixture was stirred for 8 h and filtered. The filtrate was evaporated to afford 815 mg (91%) of product as a dark brown solid: ^1H NMR (**5**, CD_3CN) δ 2.24 (4′-Me), 3.71 (4-Me), 3.83 (6-Me), 5.15 (2-H), 6.83 (3′-H), 7.14 (2′-H), 8.16 (5-H), 15.3 (SMe); absorption spectrum (acetonitrile) λ_{max} (ϵ_M) 300 (sh, 32 000), 460 (9900) nm.

(b) $(Bu_4N)_2[Fe_4S_4(LS_3)(SEt)]$ ($(Bu_4N)_2$**[6]**). The trithiol $L(SH)_3$[4] (500 mg, 0.53 mmol) was gently heated in 150 mL of dichloromethane until it dissolved. To the cooled solution was added 570 mg (0.53 mmol) of $(Bu_4N)_2[Fe_4S_4(SEt)_4]$[22] in 100 mL of acetonitrile. The reaction mixture was stirred for 30 min, and solvent was removed under dynamic vacuum to give 820 mg (85%) of product as a black solid. The ^1H NMR spectrum of the cluster in CD_3CN is virtually identical to that of its Ph_4P^+ salt.[3]

(c) $(Bu_4N)_2[Fe_4S_4(LS_3)(S\text{-}2\text{-}py)]$ ($(Bu_4N)_2$**[7]**). A solution prepared from 44.2 mg (0.024 mmol) of $(Bu_4N)_2$**[5]** in 80 mL of acetonitrile and 2.95 mg (0.027 mmol) of pyridine-2-thiol (Aldrich) in 0.5 mL of acetonitrile was stirred under dynamic vacuum for 4 h. After solvent removal, the residue was washed with toluene and dried to give the product as 38 mg (83%) of a dark brown solid: ^1H NMR (**7**, CD_3CN) δ 2.26 (4′-Me), 3.74 (4-Me), 3.92 (6-Me), 4.96 (2-H), 6.50 (py-H), 6.77 (3′-H), 7.16 (2′-H), 8.27 (5-H), 10.05 (py-H), 10.98 (py-H), 12.28 (py-H).

(d) $(Bu_4N)_2[Fe_4S_4(LS_3)(S\text{-}3\text{-}py)]$ ($(Bu_4N)_2$**[8]**). A solution of 65 mg (36 μmol) of $(Bu_4N)_2$**[5]** and 4.2 mg (38 μmol) of pyridine-3-thiol[23] in 100 mL of acetonitrile was stirred under dynamic vacuum for 3 h. The solvent was removed. The residue was washed quickly with a small amount of toluene and dried to afford the product as 62 mg (92%) of a brown solid: ^1H NMR (**8**, CD_3CN) δ 2.22 (4′-Me), 3.80 (4-Me), 3.84 (6-Me), 5.14 (2-H), 6.36 + 6.51 (py-H), 6.83 (3′-H), 7.10 (2′-H), 7.91 (py-H), 8.18 (5-H); absorption spectrum (acetonitrile) λ_{max} (ϵ_M) 300 (54 000), 352 (sh, 35 000), 480 (sh, 15 000) nm.

(e) $(Bu_4N)_2[[Fe_4S_4(LS_3)(S\text{-}4\text{-}py)]$ ($(Bu_4N)_2$**[9]**). A solution of 500 mg (0.27 mmol) of $(Bu_4N)_2$**[6]** and 30 mg (0.27 mmol) of purified pyridine-4-thiol (Aldrich) in 150 mL of acetonitrile was stirred overnight. The solvent was removed under dynamic vacuum to afford the product as 441 mg (86%) of brown solid: ^1H NMR (**9**) δ 2.22 (4′-Me), 3.83 (4-Me), 3.86 (6-Me), 5.13 (2-H), 5.89 (py-H), 6.83 (3′-H), 7.10 (2′-H), 8.19 (5-H), 8.86 (py-H); absorption spectrum (acetonitrile) λ_{max} (ϵ_M) 300 (52 000), 352 (sh, 34 000), 480 (sh, 13 000).

Ligands. (a) ***N,N′*-Ethylenebis(trifluoroacetylacetonelmine) (H_2(tfacen)).** A published procedure[24] was modified. A solution of 15.4 g (100 mmol) of 1,1,1-trifluoropentane-2,4-dione in 60 mL of ethanol was treated with 3.0 g (50 mmol) of ethylenediamine in 30 mL of ethanol. The solution was refluxed for 30 min and cooled to 0 °C in an ice bath,

(16) Huynh, B. H.; Kang, L.; DerVartanian, D. V.; Peck, H. D., Jr.; LeGall, J. *J. Biol. Chem.* **1984**, *259*, 15373.
(17) Cowan, J. A.; Sola, M. *Inorg. Chem.* **1990**, *29*, 2176.
(18) Pierik, A. J.; Hagen, W. R. *Eur. J. Biochem.* **1991**, *195*, 505.
(19) Young, L. J.; Siegel, L. M. *Biochemistry* **1988**, *27*, 2790, 5984.
(20) Wilkerson, J. O.; Janick, P. A.; Siegel, L. M. *Biochemistry* **1983**, *22*, 5048.
(21) Challen, P. R.; Koo, S.-M.; Dunham, W. R.; Coucouvanis, D. *J. Am. Chem. Soc.* **1990**, *112*, 2455.
(22) Averill, B. A.; Herskovitz, T.; Holm, R. H.; Ibers, J. A. *J. Am. Chem. Soc.* **1973**, *95*, 3523.
(23) Fürst, H.; Helizig, M.; Göbel, W. *J. Prakt. Chem.* **1967**, *36*, 1967.
(24) Martell, A. E.; Belford, R. L.; Calvin, M. *J. Inorg. Nucl. Chem.* **1958**, *5*, 170.

and ice-cold water (100 mL) was added. The crude product obtained by maintaining the reaction mixture at 0 °C overnight was recrystallized from 60% ethanol/water (v/v) to afford 12.0 g (80%) of product as colorless needle crystals: ^{1}H NMR ($CDCl_3$) δ 2.06, 2.09 (6); 5.37 (2); 3.64, 3.62 (4); 11.2 (2).

(b) *N,N'*-2,6-Diethylpyridinebis(trifluoroacetylacetoneimine) (H_2-(tfacenpy)). A solution of 3.5 g (21 mmol) of 2,6-bis(aminoethyl)-pyridine[25] in 20 mL of ethanol was added to a solution of 6.53 g (42 mmol) of 1,1,1-trifluoro-2,4-pentanedione in 20 mL of ethanol. The mixture was heated under reflux for 1 h, the volume of the solution was reduced to 15 mL, and the solution was maintained at −20 °C overnight. After filtration and washing with cold ethanol, the product was obtained as 4.1 g (45%) of light yellow solid: mp 114–116 °C. ^{1}H NMR ($CDCl_3$) δ 2.03 (s, 6), 3.10 (t, 4), 3.83 (q, 4), 5.24 (s, 2), 7.04 (d, 2), 7.56 (t, 1), 11.3 (br, 2); FAB-MS (3-nitrobenzyl alcohol) $[M + H]^+$ 438. Anal. Calcd for $C_{19}H_{21}F_6N_3O_2$: C, 52.18; H, 4.84; N, 9.61. Found: C, 52.19; H, 4.77; N, 9.48.

Iron(II) Complexes. (a) $FeCl_2$·1.5THF. This starting compound was prepared by a more convenient method than those reported.[26,27] A slurry of 7.00 g (55.2 mmol) of anhydrous $FeCl_2$ in 150 mL of THF was stirred at 50 °C for 3 h, during which solid changed from light yellow to white. After the mixture was maintained at −20 °C overnight, it was filtered to give 11.80 g (91%) of product as a white solid: Anal. Calcd for $C_6H_{12}Cl_2FeO_{1.5}$: C, 30.68; H, 5.15; Cl, 30.18. Found: C, 29.40; H, 4.69; Cl, 30.25.

(b) [Fe(acen)]. The previously reported synthesis of this compound[27] has been altered to reduce formation of the μ-oxo Fe(III) contaminant. A slurry of 1.00 g (4.46 mmol) of H_2(acen)[28] and 1.05 g (4.46 mmol) of $FeCl_2$·1.5THF in 80 mL of THF was stirred for 2 h, during which a yellow solid formed. The mixture was treated with 0.48 g (8.92 mmol) of freshly prepared NaOMe, refluxed for 2 h, and filtered. Removal of solvent from the filtrate gave a red-green solid, which was washed with hot acetonitrile and then dried to afford the product as 1.0 g (82%) of a greenish-yellow solid: ^{1}H NMR (CD_3CN) δ −58.1 (Me), −35.3 (Me) −17.2 (CH). 82.4 (CH_2CH_2).

(c) [Fe(acen)(py)]. This compound[27] was obtained by a procedure analogous to that for [Fe(tfacen)(py)$_2$] (below). Its ^{1}H NMR spectrum is identical with that obtained from the addition of pyridine to Fe(acen) at the same concentration.

(d) [Fe(tfacen)(py)$_2$]. To a solution of 1.0 g (3.0 mmol) of H_2(tfacen) in 10 mL of methanol and 20 mL of acetonitrile was added 0.32 g (6.0 mmol) of freshly prepared NaOMe in 5 mL of methanol. The mixture was stirred for 30 min at 50 °C and 12 mL (150 mmol) of pyridine was added. Addition of 0.38 g (3.0 mmol) of $FeCl_2$ in 10 mL of methanol caused an instant color change to dark red. The reaction mixture was stirred for 2 h at 60 °C, maintained near 0 °C overnight, and filtered. The filtrate volume was reduced to 15–20 mL in vacuo and stored at −20 °C for 12 h. The solid was collected, washed with hexanes, and dried to afford the product as 1.0 g (61%) of dark red crystals. Anal. Calcd for $C_{22}H_{22}F_6FeN_4O_2$: C, 48.55; H, 4.07; N, 10.29. Found: C, 48.25; H, 4.03; N, 10.20.

(e) [Fe(tfacen)(MeCN)]. The preceding preparation was followed up to the 60 °C/2 h stirring step but with the omission of pyridine. The reaction mixture was cooled, the solvent was removed in vacuo, and 100 mL of acetonitrile was added to the residue. The mixture was stirred at 40 °C for 30 min, placed in an ice bath for 1 h, and filtered to remove NaCl, and the solvent was removed from the filtrate in vacuo. The solid residue was washed with hot hexanes and dried to give the product as 1.0 g (80%) of a brown solid. The compound was pure by its ^{1}H NMR spectrum, which is concentration dependent in CD_2Cl_2; signal intensities established the 1:1 adduct formulation: ^{1}H NMR (CD_2Cl_2, 0.11 M) δ −59.7 (Me), −17.1 (MeCN), −11.7 (CH), 69.1 (CH_2CH_2).

(f) [Fe(tfacenpy)]. To a solution of 250 mg (0.57 mmol) of H_2(tfacenpy) in 15 mL of ethanol was added a solution of 62 mg (1.14 mmol) of freshly prepared NaOMe in 5 mL of methanol. The solution was stirred at 50 °C for 30 min, and 72 mg (0.57 mmol) of $FeCl_2$ in 15 mL of acetonitrile was added, giving a red solution. The reaction mixture was stirred for 12 h, and the solvent was taken off in vacuo. Sodium chloride was removed as in the preceding preparation, the volume of the acetonitrile filtrate was reduced to 15–20 mL, and this solution was allowed to stand for 12 h at room temperature. The product was collected as 225 mg (85%) of red crystals: FAB-MS (3-nitrobenzyl alcohol) M^+ 491, $[M + H]^+$ 492. Anal. Calcd for $C_{19}H_{19}F_6FeN_3O_2$: C, 46.46; H, 3.90; N, 8.55. Found: C, 46.34; H, 3.82; N, 8.47.

Bridged Assemblies. (a/b) $(Bu_4N)_2$[$Fe_4S_4(LS_3)$(S-3/4-py-Fe(acen))] ($(Bu_4N)_2$[8-Fe(acen)/9-Fe(acen)]). These two compounds were isolated by similar means. The procedure for the second is given. A solution of 190 mg (0.10 mmol) of $(Bu_4N)_2$[**9**] and 45 mg (0.16 mmol) of Fe(acen) in 20 mL of acetonitrile was stirred for 1 h. The solvent was evaporated, and the residue was recrystallized from acetonitrile/toluene. The solid was collected by filtration and dried in vacuo to yield the product as 140 mg (64%) of a dark brown microcrystalline solid.

(c) $(Bu_4N)_2$[$Fe_4S_4(LS_3)$(S-4-py-Fe(tfacen))] ($(Bu_4N)_2$[9-Fe(tfacen)]). This species was generated in solution but was not isolated. A solution of 6.35 mg (14.9 μmol) of Fe(tfacen)(MeCN) in 0.2 mL of acetonitrile was added to a solution of 28.2 mg (14.9 μmol) of $(Bu_4N)_2$[**9**] in 0.5 mL of acetonitrile, and the mixture was stirred for 20 min.

The ^{1}H NMR spectra of the three bridged species are concentration-dependent and are discussed in the text.

X-ray Structural Determinations. Dark red crystals of Fe(tfacen)(py)$_2$ were grown from a solution of the compound in methanol/acetonitrile/pyridine (1:1:1 v/v) at room temperature. Orange-red crystals of Fe(tfacenpy) were obtained from the preparative procedure. The crystals were sealed in glass capillaries. Data were collected on a Nicolet P3 automated diffractometer equipped with Nb filter and using Mo Kα radiation. The unit cell parameters were determined from 25 reflections in the ranges $15.2 \le 2\theta \le 30.3°$ for Fe(tfacen)(py)$_2$ and $18.1 \le 2\theta \le 33.9°$ for Fe(tfacenpy). Systematic absences established the space group of the former compound as tetragonal $P4_2/n$ and of the latter as monoclinic $C2/c$ or Cc. The structure was successfully refined only in $C2/c$. Diffraction data were processed with the SHELXTL PLUS program package (Siemens XRD Corporation, Madison, WI 53711). A numerical absorption correction was applied to Fe(tfacen)(py)$_2$ and an empirical absorption correction to Fe(tfacenpy). All non-hydrogen atoms were located by direct methods and XP-interactive graphical editing. Isotropic refinements of Fe(tfacen)(py)$_2$ and Fe(tfacenpy) converged at $R = 13.8\%$ and 11.5%, respectively. In the final stages of anisotropic refinement, hydrogen atoms were introduced at 0.96 Å from, and with 1.3× the isotropic thermal parameters of, bonded carbon atoms. Crystallographic data and unweighted and weighted R factors are given in Table I.[29]

Physical Measurements. All measurements were performed under anaerobic conditions. Absorption spectra were recorded on a Perkin-Elmer Lambda C spectrophotometer. ^{1}H NMR spectra were measured at 297 K on a Bruker AM-500 spectrometer. Cyclic voltammograms were recorded at 100 mV/s in acetonitrile solutions containing 0.2 M $(Bu_4N)(PF_6)$ supporting electrolyte. Standard PAR equipment with a Pt working electrode and a SCE reference electrode were employed. Under the conditions used, $E_{1/2} = 0.42$ V for the $[Cp_2Fe]^{1+,0}$ couple in acetonitrile.

Table I. Crystallographic Data[a] for Fe(tfacen)(py)$_2$ and Fe(tfacenpy)

	Fe(tfacen)(py)$_2$	Fe(tfacenpy)
formula	$C_{22}H_{22}F_6FeN_4O_2$	$C_{19}H_{19}F_6FeN_3O_2$
formula wt	544.28	491.22
a, Å	12.698 (4)	14.351 (2)
b, Å	12.698 (4)	10.969 (1)
c, Å	14.839 (4)	14.385 (2)
space group	$P4_2/n$	$C2/c$
Z	4	4
V, Å^3	2392 (2)	2010.8 (4)
T, K	200	298
$\rho_{calcd}(\rho_{obs})$, g/cm^3	1.51 (1.49)[b]	1.62 (1.62)[c]
μ, cm^{-1}	7.0	8.2
$R(R_w)$, %	4.6 (4.7)	3.6 (4.1)

[a] λ = 0.71073 Å (Mo Kα). [b] Determined by flotation in benzene/CCl_4. [c] Determined by flotation in 1,3-dibromopropane/hexane.

Results and Discussion

Preparation of Subsite-Functionalized Clusters. The clusters **1** present the considerable advantage of subsite-specific ligand substitution reactions, thereby avoiding mixtures of products potentially or actually formed with clusters lacking subsite differentiation.[2] With reference to Figure 1, site-differentiated clusters **5** and **6** are the precursors to all other cluster species examined in this work. They are readily obtained in high yield

(25) Chen, D.; Martell, A. E.; Sun, Y. *Inorg. Chem.* **1989**, *28*, 2647.
(26) Bel'skii, V. K.; Ishchenko, V. M.; Bulychev, B. M.; Protskii, A. N.; Soloveichik, G. L.; Ellert, O. G.; Seifulina, Z. M.; Rakitin, Yu. V.; Novotortstev, V. M. *Inorg. Chim. Acta* **1985**, *96*, 123.
(27) Corazza, F.; Floriani, C.; Zehnder, M. *J. Chem. Soc., Dalton Trans.* **1987**, 709.
(28) Martin, D. F.; Olszewski, E. J. *Inorg. Synth.* **1966**, *8*, 46.
(29) See the paragraph at the end of this article concerning supplementary material available.

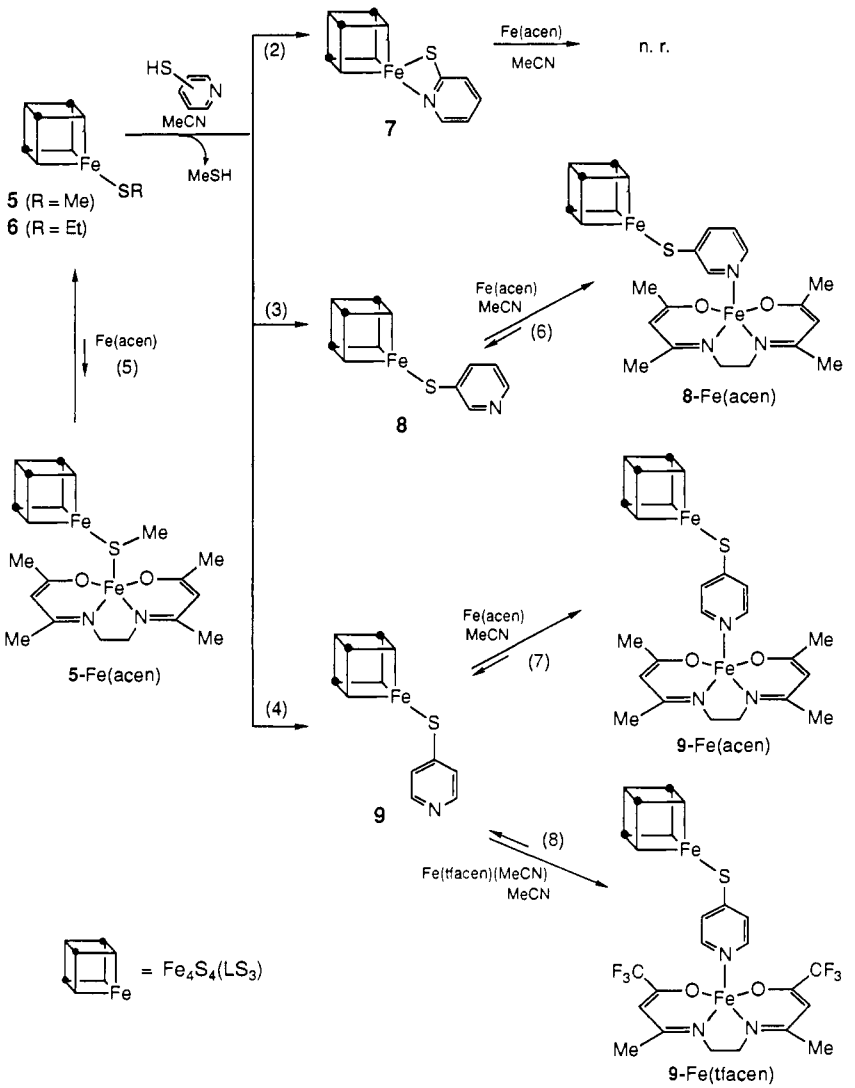

Figure 1. Schematic representations of equilibrium reaction 5, preparation of subsite-functionalized *S*-pyridyl clusters **7**–**9** in reactions 2–4, and formation of bridged assemblies **8**/**9**-Fe(acen) and **9**-Fe(tfacen) in equilibrium reactions 6–8. All reactions were carried out in acetonitrile solutions.

as Bu_4N^+ salts by reaction 1 (R = Me, Et), which is conducted under dynamic vacuum to remove the liberated alkylthiol. The ^{1}H NMR spectrum of **5** shown in Figure 2 demonstrates the purity

$$[Fe_4S_4(SR)_4]^{2-} + L(SH)_3 \rightarrow [Fe_4S_4(LS_3)(SR)]^{2-} + 3RSH \quad (1)$$

of the cluster; **6** has been obtained in equivalent purity. Signal assignments were made as for related clusters **1**[3] using the indicated atom numbering scheme. Clusters containing the $[Fe_4S_4]^{2+}$ core exhibit small isotropic shifts that are extremely sensitive to the nature of the ligand at the unique subsite.[3,7,9] For example, in acetonitrile solution the 5-H shift of chloride cluster **2** is 8.23 ppm, whereas thiolate clusters **3** show this signal at 8.10–8.18 ppm. The shifts of the other ring substituents in the coordinating arms of **1** also respond sensitively to ligand variation at the unique subsites, whereas resonances of the legs are generally much less affected.

Treatment of **5** or **6** with the three isomeric pyridinethiols in equimolar amount or slight excesses in reactions 2–4 yields the corresponding clusters **7**–**9** (Figure 1). These reactions were carried out under dynamic vacuum to remove liberated alkylthiol and afforded pure products without recrystallization. The ^{1}H NMR spectra of **8** and **9**, shown in Figure 2, are consistent with the indicated structures. The SMe or SEt signals of precursor **5** (15.3 ppm) or **6** (2.37, 13.2 ppm) are absent. Thiolate ligation is supported by the 5-H shifts of 8.18–8.19 ppm. Three pyridine proton signals are resolved for **8** and two are evident for **9**. For the former, the signal at 7.91 ppm is twice the intensity of those at 6.36 and 6.51 ppm. In CD_2Cl_2 solution, this resonance is split into two equally intense signals at 7.87 and 7.95; the remaining pyridine proton resonances occur at 5.93 (br) and 6.39 ppm. In the spectra of **8** and **9**, the signal assignments py-$H_{\alpha,\gamma}$ and py-H_β, respectively, are made on the basis of line width, these protons being nearest the paramagnetic cluster core. Other py-H signals of **8** cannot be securely assigned. The spectrum of the pyridine ring portion of cluster **7** (not shown) is completely different. Three signals are shifted strongly downfield (10.05, 10.98, 12.68 ppm) and a fourth resonance is observed at 6.50 ppm. This spectrum has been encountered previously in the reaction product of **2** and Na(S-2-py) in acetonitrile solution, which was isolated as its Ph_4P^+ salt.[7] That method of preparation eliminates ligand coordination as 1*H*-pyridine-2-thione, a known binding mode of the neutral ligand.[30,31] These spectral differences support the indicated ring structure for **7**. The ability of pyridine-2-thiolate to support stable chelate rings has been amply demonstrated.[31,32]

(30) (a) Raper, E. S. *Coord. Chem. Rev.* **1985**, *61*, 115. (b) Valle, G.; Ettorre, R.; Vettori, U.; Peruzzo, V.; Plazzogna, G. *J. Chem. Soc., Dalton Trans.* **1987**, 815. (c) Deeming, A. J.; Hardcastle, K. I.; Meah, M. N.; Bates, P. A.; Dawes, H. M.; Hursthouse, M. B. *J. Chem. Soc., Dalton Trans.* **1988**, 227.

(31) Mura, P.; Olby, B. G.; Robinson, S. D. *J. Chem. Soc., Dalton Trans.* **1985**, 2101, and references therein.

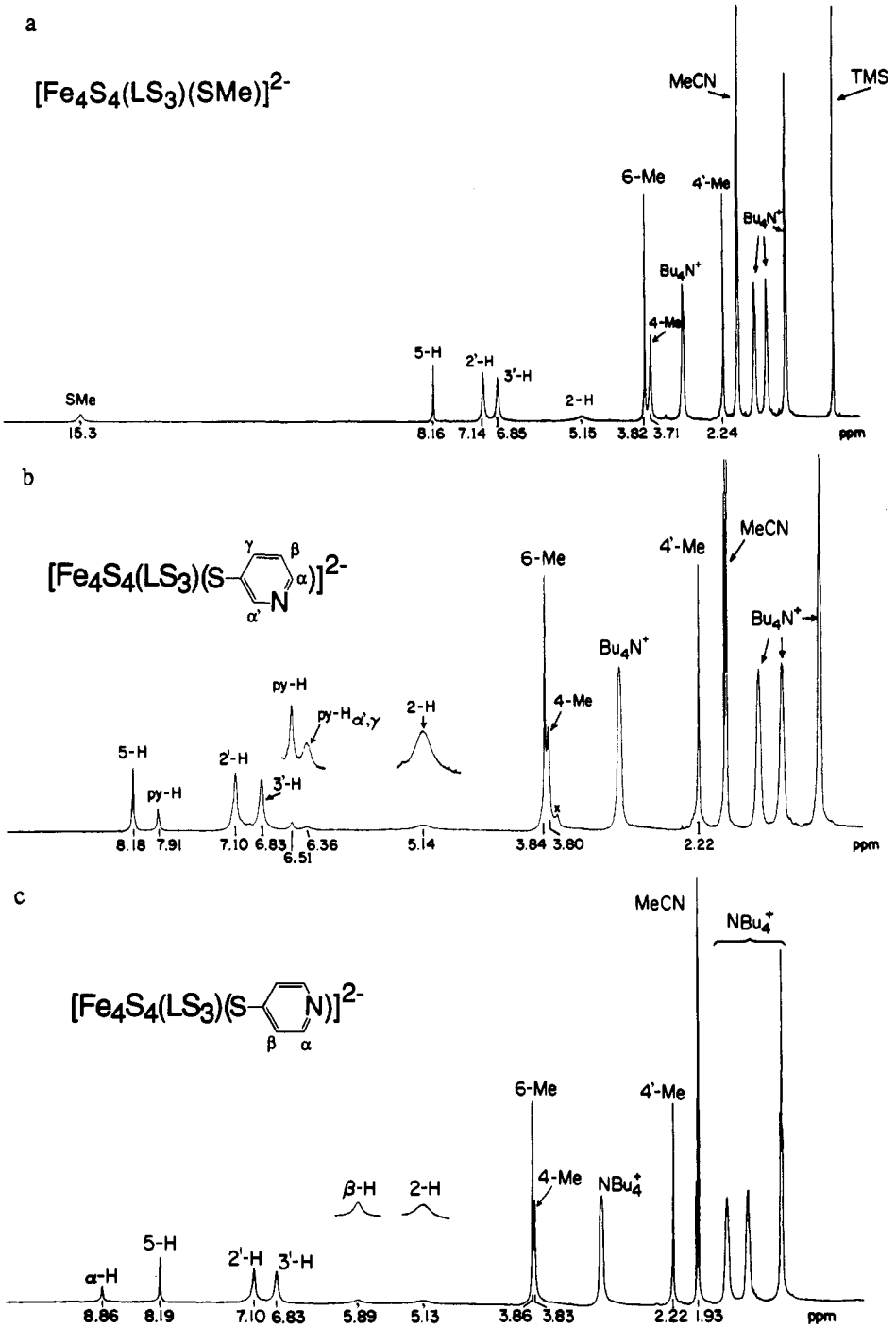

Figure 2. ^1H NMR spectra in CD_3CN solutions at 297 K: (A) $[Fe_4S_4(LS_3)(SMe)]^{2-}$ (**5**), (B) $[Fe_4S_4(LS_3)(S\text{-}3\text{-}py)]^{2-}$ (**8**), and (C) $[Fe_4S_4(LS_3)(S\text{-}4\text{-}py)]^{2-}$ (**9**). Signal assignments are indicated. The spectrum of $[Fe_4S_4(LS_3)(S\text{-}2\text{-}py)]^{2-}$ (**7**) is available elsewhere.[7]

Preparation of Bridged Assemblies. In seeking to connect an Fe_4S_4 cluster with an iron complex, a number of bridging modes to various types of complexes can be conceived. In this initial phase of constructing bridged assemblies, we describe reactions with Fe(acen) and Fe(tfacen), quadridentate complexes selected because of favorable solubility properties, the apparent lack of any significant steric impediment to axial ligand binding, affinities for nitrogenous and thiolate axial ligands as shown by the isolation of Fe(acen)(py),[27] Na[Fe(acen)(SMe)],[33] and Fe(tfacen)$(py)_2$, and clean electrochemical oxidation to the Fe(III) state when axially ligated. Fe(acen) is a dimer in the crystalline state but a monomer in freezing benzene; it ($4.84\mu_B$) and its pyridine adduct ($4.95\mu_B$) have $S = 2$ in the solid state.[27] This spin state is maintained by Fe(acen) ($4.7\mu_B$) and Fe(acen)(py) ($4.8\mu_B$) in acetonitrile solution. From comparable isotropic shifts, we conclude that Fe(tfacen)(MeCN) and its pyridine complexes also have $S = 2$. All reactions described in the following sections were carried out at ambient temperature in acetonitrile solutions.

(a) Methanethiolate-Bridged. Reaction of Fe(acen) and cluster **5** (selected for minimum steric hindrance) resulted in the equilibrium 5 in Figure 1. Chemical shifts of both components were found to depend on their concentration ratios over the range [Fe(acen)]:[**5**] = 1:1–5:1, at which fast exchange prevails. (Significantly higher ratios were limited by the solubility of Fe(acen).) For example, at 5:1 and [**5**] = 5.6 mM, the SMe res-

(32) (a) Rosenfeld, S. G.; Swedberg, S. A.; Arora, S. K.; Mascharak, P. K. *Inorg. Chem.* **1986**, *25*, 2109. (b) Rosenfeld, S. G.; Berends, H. P.; Gelmini, L.; Stephan, D. W.; Mascharak, P. K. *Inorg. Chem.* **1987**, *26*, 2792.

(33) This compound was prepared by the reaction of Fe(acen) with excess (1.9 equiv) of NaSMe in acetonitrile and obtained as an orange solid: ^1H NMR (CD_3CN, 297 K) δ −14.0 (CH), −20.8 (Me), −32.8 (Me); the SMe and CH_2 signals are very broad and accurate shifts were not obtained.

onance is shifted downfield to 16.1 from 15.3 ppm (Figure 2) in the absence of Fe(acen). This and other observations indicated the presence of a labile equilibrium, in which the new paramagnetic component is plausibly the bridged assembly **5**-Fe(acen). The reaction did not result in the irreversible transfer of MeS^- to Fe(acen) inasmuch as the NMR signals of $[Fe(acen)(SMe)]^{1-}$[33] were not observed. In the reaction of equimolar $[Fe_4S_4(SPh)_4]^{2-}$ and Fe(OEP)X in acetonitrile, either Fe(OEP)(SPh) or Fe(OEP) was obtained in good yield depending on the solvent.[34] Because reaction 5 lies heavily toward the separate components, it has not been characterized further. A more electrophilic Fe(II) complex and retention of a small R substituent in the μ-SR group are required to stabilize a thiolate-bridged product. A less labile bridge between cluster and complex was next sought.

(b) Pyridinethiolate-Bridged. No complexes of pyridine-3-thiol have been reported. A limited number of complexes of pyridine-4-thiol are known, but coordination occurs at the sulfur atom in the thione form.[30] When present in functionalized clusters **8** and **9**, these ligands present potential pyridyl nitrogen ligating sites that are expected to have stronger binding affinities than the methanethiolate group of **5**. Reactions 6 and 7 (Figure 1) proceed readily in acetonitrile solutions to afford in reasonable isolated yield new products that have been identified from spectroscopic and electrochemical data as the bridged assemblies **8**-Fe(acen) and **9**-Fe(acen). Reactions of equimolar components in acetonitrile solution result in the generation of species with ^1H NMR spectra identical to those of the isolated products at the same concentration. The species **9**-Fe(tfacen) was generated in acetonitrile solution in this way by reaction 8. Cluster **7** and Fe(acen), each at 120 mM, did not react over a period of at least 10 h, a result consistent with the chelate structure of the cluster.

Demonstration of the formation of bridged species **9**-Fe(acen) and **9**-Fe(tfacen) follows from the ^1H NMR spectra in Figures 3 and 4, respectively. These should be compared with the spectra of cluster **9** (Figure 2) and Fe(acen)(py) (Figure 3) and Fe(tfacen)$(py)_2$ (Figure 4). The chemical shifts of all pyridine adduct species are concentration-dependent, signifying equilibrium reactions, which have been analyzed (vide infra). At this point, the spectra are utilized to demonstrate the formation of bridged assemblies, including also **8**-Fe(acen) (spectrum not shown). Chemical shifts in all three portions of the products, the cluster, bridge, and iron complex, are affected. Observations refer to species in the 3–30 mM concentration range.

(i) **Clusters.** The shifts of all LS_3 signals of cluster **8** are significantly altered, being displaced upfield by 0.13–0.45 ppm in the formation of **8**-Fe(acen). The corresponding shifts of **9** undergo much smaller changes, the major effects being a 0.05 ppm upfield shift of 6-Me and a 0.18 ppm downfield shift of 4-Me upon reaction with Fe(acen). Small but definite shift changes are also observed in the formation of **9**-Fe(tfacen).

(ii) **Bridges.** Pyridine proton signals in the 6–9 ppm range for **8** and **9** are abolished and are replaced by new signals at 21.5 and 35.8 (**8**-Fe(acen)), 28.1 (**9**-Fe(acen)), and 27.7 ppm (**9**-Fe(tfacen)). These values are in the range of, but different from, the β-H shifts of the pyridine adducts of the Fe(II) complexes. The two resonances in **8**-Fe(acen) cannot be individually assigned but are attributed to $H_{\beta,\gamma}$. Signals corresponding to α-H and expected near ca. 90 ppm are presumably broadened beyond detection in the accessible concentration range.

(iii) **Fe(II) Complexes.** Taking the spectra of Fe(acen) and Fe(tfacen)(MeCN) as references, upfield shifts of 2–12 (Me) and 2–6 (CH) ppm are characteristic of the binding of one pyridine-type ligand to the two Fe(II) complexes. Shifts of the acen and tfacen methyl and methine protons in the bridged species clearly occur close to or within the ranges found for Fe(acen)(py) and Fe(tfacen)$(py)_{1,2}$ (vide infra). The values of these shifts, and those of pyridine β-H resonances, demonstrate the $S = 2$ spin state of the Fe(acen) and Fe(tfacen) units in the bridged products.

The foregoing results convincingly demonstrate axial binding of the pyridyl groups in clusters **8** and **9** by the Fe(II) complexes to form the bridged assemblies **8**/**9**-Fe(acen) and **9**-Fe(tfacen). These species retain the $S = 0$ and $S = 2$ ground states of the separate cluster and Fe(II) complex, respectively. The NMR spectra are consistent with average trigonal symmetry in solution. The relatively large shift changes noted in (i) for **8**-Fe(acen) suggest an average configuration in which cluster and complex are in closer proximity than in **9**-Fe(acen)/Fe(tfacen). As yet, diffraction-quality crystals of the bridged species have not been obtained.

Table II. Formation Constants of Fe(II)–Pyridine Complexes and Bridged Assemblies

species	K_{f1} (M^{-1})	K_{f2} (M^{-1})	limiting shifts (ppm)[b] δ_1, δ_2	ref
Fe(acen)(py)	330		26.1	*a*
Fe(tfacen)(py)	450	40	27.8, 36.3	*a*
9-Fe(acen)	790		33.5	*a*
9-Fe(tfacen)	920	*f*	32.9	*a*
Fe(Cap)(py)[c]	76			38
Fe(TPP)$(py)_2$[d]	1500	1.9×10^4		35c
Fe(HmCap)$(py)_2$[c]	148	6.9		38
Fe(Pc)$(py)_2$[e]	1260	76		37

[a] This work, acetonitrile solution. [b] Pyridine β-H. [c] Toluene solution. [d] Benzene solution. [e] Me_2SO solution. [f] Not determined.

Equilibria of Bridged Assemblies. As indicated above, the bridged assemblies in Figure 1 exist in equilibrium with their components in reactions 6–8. These reactions are related to others involving the binding of nitrogenous ligands to Fe(II) macrocycles whose equilibria[35–38] and kinetics[39] have been examined. The difficulties in evaluating equilibrium constants in such cases have been noted.[38] Such equilibria may intervene in the solution behavior of various types of bridged assemblies. Consequently, we have developed an NMR method, outlined in the Appendix, for the determination of one or of two stepwise binding constants. The method utilizes NMR chemical shifts at fast exchange as a concentration monitor, an approach that is facilitated here by large isotropic shifts and attendant appreciable shift differences between species in equilibrium. All reaction systems were monitored with the averaged β-H shift ($\delta_{\beta H}$) of pyridine in view of the ca. 7–30 ppm difference between free and coordinated pyridine.

(a) Fe(II) Complex/Pyridine Systems. The method was first applied to pyridine binding by Fe(acen) and Fe(tfacen) in reactions 9 (L′ = acen, tfacen) and 10 (L′ = tfacen), with equilibrium constants 11 and 12, respectively. Formation constants determined in acetonitrile solutions are set out in Table II together with values of the chemical shifts of bound pyridine calculated from the analysis.

$$FeL' + py \rightleftharpoons FeL'(py) \quad (9)$$

$$FeL'(py) + py \rightleftharpoons FeL'(py)_2 \quad (10)$$

$$K_{f1} = [FeL'(py)]/[FeL'][py] \quad (11)$$

$$K_{f2} = [FeL'(py)_2]/[FeL'(py)][py] \quad (12)$$

The system Fe(acen)/py is described by the simple equilibrium 9 with formation constant $K_f = 330\ M^{-1}$. The ^1H NMR spectra

(34) Stolzenberg, A. M.; Stershic, M. T. *Inorg. Chem.* **1985**, *24*, 3098.

(35) (a) Rougee, M.; Brault, D. *Biochem. Biophys. Res. Commun.* **1973**, *55*, 1364. (b) Brault, D.; Rougee, M. *Biochem. Biophys. Res. Commun.* **1974**, *57*, 654. (c) Brault, D.; Rougee, M. *Biochemistry* **1974**, *13*, 4591. (d) Rougee, M.; Brault, D. *Biochemistry* **1975**, *14*, 4100.

(36) Collman, J. P.; Brauman, J. I.; Doxsee, K. M.; Halbert, T. R.; Suslick, K. S. *Proc. Natl. Acad. Sci. U.S.A.* **1978**, *75*, 564.

(37) Kadish, K. M.; Bottomley, L. A.; Cheng, J. S. *J. Am. Chem. Soc.* **1978**, *100*, 2731.

(38) Ellis, P. E., Jr.; Linard, J. E.; Szymanski, T.; Jones, R. D.; Budge, J. R.; Basolo, F. *J. Am. Chem. Soc.* **1980**, *102*, 1889.

(39) (a) Hamilton, D. E.; Lewis, T. J.; Kildahl, N. K. *Inorg. Chem.* **1979**, *18*, 3364. (b) Martinsen, J.; Miller, M.; Trojan, D.; Swelgart, D. *Inorg. Chem.* **1980**, *19*, 2162. (c) Kildahl, N. K.; Lewis, T. J.; Antonopoulos, C. *Inorg. Chem.* **1981**, *20*, 3952. (d) Kildahl, N. K.; Balkus, K. J., Jr.; Flynn, M. *Inorg. Chem.* **1983**, *22*, 589. (e) Butler, A.; Linck, R. G. *Inorg. Chem.* **1984**, *23*, 4545. (f) Kildahl, N. K.; Antonopoulos, G.; Fortier, N. E.; Hobey, W. D. *Inorg. Chem.* **1985**, *24*, 429. (g) Chen, X.; Stynes, D. V. *Inorg. Chem.* **1986**, *25*, 1173. (h) Siddiqui, N.; Stynes, D. V. *Inorg. Chem.* **1986**, *25*, 1982.

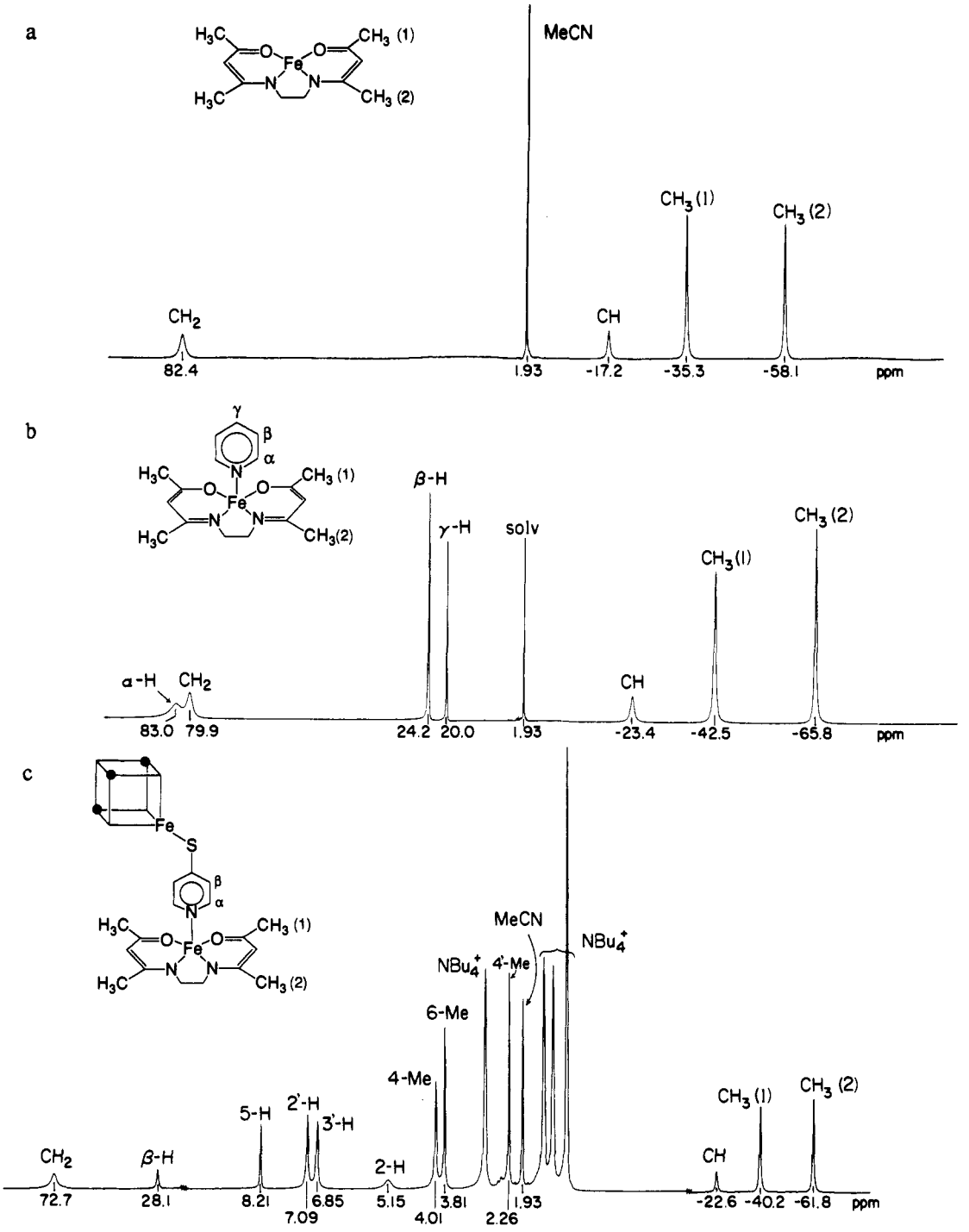

Figure 3. ^1H NMR spectra in CD_3CN solutions at 297 K (A) Fe(acen), (B) Fe(acen)(py) (90%, [Fe] = 0.269 M), and (C) bridged species 9-Fe(acen) (80%), generated from its components each at 25.2 mM. Signal assignments are indicated; the percents in this and the following figure refer to the amount of solute species in the specified form. Chemical shift scales are not constant; note the scale breaks just after 28 ppm and just before −22 ppm in spectrum c.

of the two Fe(II) complexes are compared in Figure 3; at the indicated concentration the extent of formation of Fe(acen)(py) is 90%. Shown in Figure 5A is a comparison of the observed values of $\delta_{\beta H}$ over a range of total Fe concentration, and those calculated from the equilibrium constant and the limiting value $\delta_1 = \delta_{\beta H}$ for Fe(acen)(py). The agreement is highly satisfactory.

In relation to the Fe(tfacen)/py system, we have been unable to prepare Fe(tfacen) itself, but we have isolated Fe(tfacen)-(MeCN). The ^1H NMR spectrum of this compound in CD_2Cl_2 solution, shown in Figure 4A, reveals an isotropically shifted methyl signal of coordinated acetonitrile at −16.8 ppm. When treated with a small excess of pyridine, the coordinated acetonitrile is liberated. In acetonitrile solution bound and free acetonitrile are in fast exchange, and methyl and methine chemical shifts are independent of concentration. This system is interpreted in terms of equilibria 9 and 10. To allow comparison of equilibrium constants with the Fe(acen)/py system, in which the extent of solvation of Fe(acen) is unknown, coordinated acetonitrile is not included in reaction 9. We find $K_{f1} = 450\ M^{-1}$, some 36% larger than for Fe(acen),[40] a behavior induced by the electron-withdrawing effect of the two trifluoromethyl groups. It was because of the possibility of tighter ligand binding that the reactions of the tfacen complex were examined. Agreement as good as that

(40) Scaringe, R. P.; Hodgson, D. J. *Inorg. Chem.* **1976**, *15*, 1193.

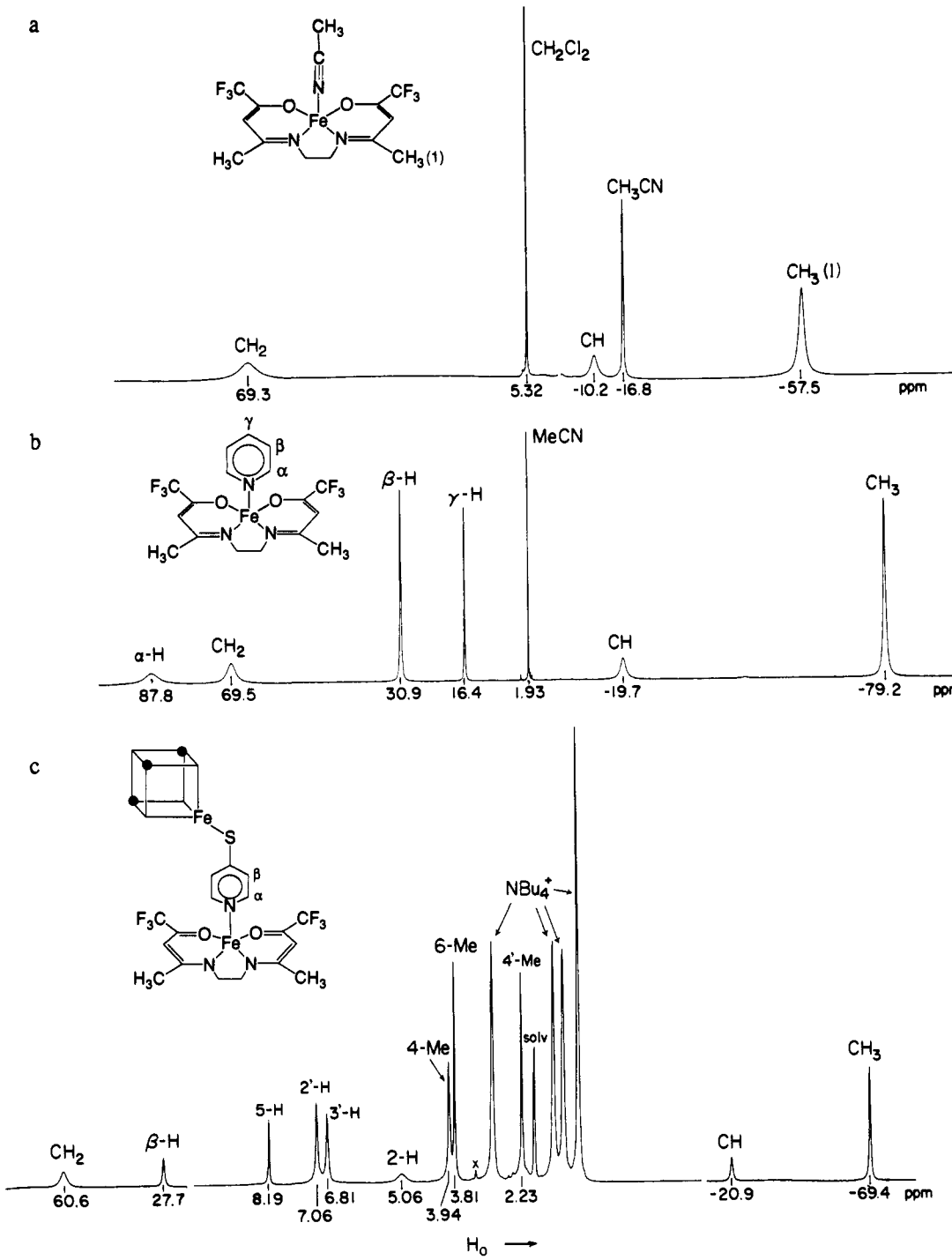

Figure 4. ^{1}H NMR spectra in CD_3CN solutions at 297 K (A) Fe(tfacen)(MeCN) in CD_2Cl_2, (B) Fe(tfacen)(py) (28%) + Fe(tfacen)$(py)_2$ (71%) ([Fe] = 0.210 M), and (C) bridged species **9**-Fe(tfacen) (80%), generated from its components each at 21.4 mM. Signal assignments are indicated. Chemical shift scales are not constant; note the scale breaks just after 27 ppm and just before −20 ppm in spectrum c.

in Figure 5A was obtained between calculated and observed values of $\delta_{\beta H}$.

The tendency of Fe(tfacen) to bind a second pyridine, as reflected by K_{f2} = 40 M^{-1}, is small. However, in the presence of excess pyridine in methanol Fe(tfacen)$(py)_2$ is readily crystallized. Its structure is shown in Figure 6, and selected dimensions are listed in Table III. The molecule has trans stereochemistry, with an imposed 2-fold axis that bisects the O–Fe–O angle, an essentially planar FeO_2N_2 equatorial coordination unit, and two axial pyridine rings disposed at a dihedral angle of 78.1°. Ligand dimensions are quite similar to those of Ni(tfacen).[40] The ethylene bridge is in the gauche conformation, with carbon atoms 0.34 Å above and below the equatorial coordination plane. The pyridine rings are oriented so as to reduce the interaction of α-hydrogens with the bridge hydrogen atoms.

(b) Bridged Assemblies. Equilibrium constants for the cluster assembly reactions 7 and 8 are defined analogously to eq 11. Owing to solubility limitations, these reactions were examined in

$$[Fe_4S_4(LS_3)(S\text{-}4\text{-}py)]^{2-} + Fe(acen) \rightleftharpoons \mathbf{9}\text{-}Fe(acen) \quad (7)$$

$$[Fe_4S_4(LS_3)(S\text{-}4\text{-}py)]^{2-} + Fe(tfacen) \rightleftharpoons \mathbf{9}\text{-}Fe(tfacen) \quad (8)$$

solutions relatively dilute compared to reactions 9 and 10. The values K_f = 790 M^{-1} for reaction 7 and 920 M^{-1} for reaction 8 are in the same order as for reaction 9, but the tfacen ligand provides only a 16% binding enhancement. However, the equilibrium constants are higher than for reaction 9, a matter we attribute to a resonance contribution of the pyridine-4-thiolate

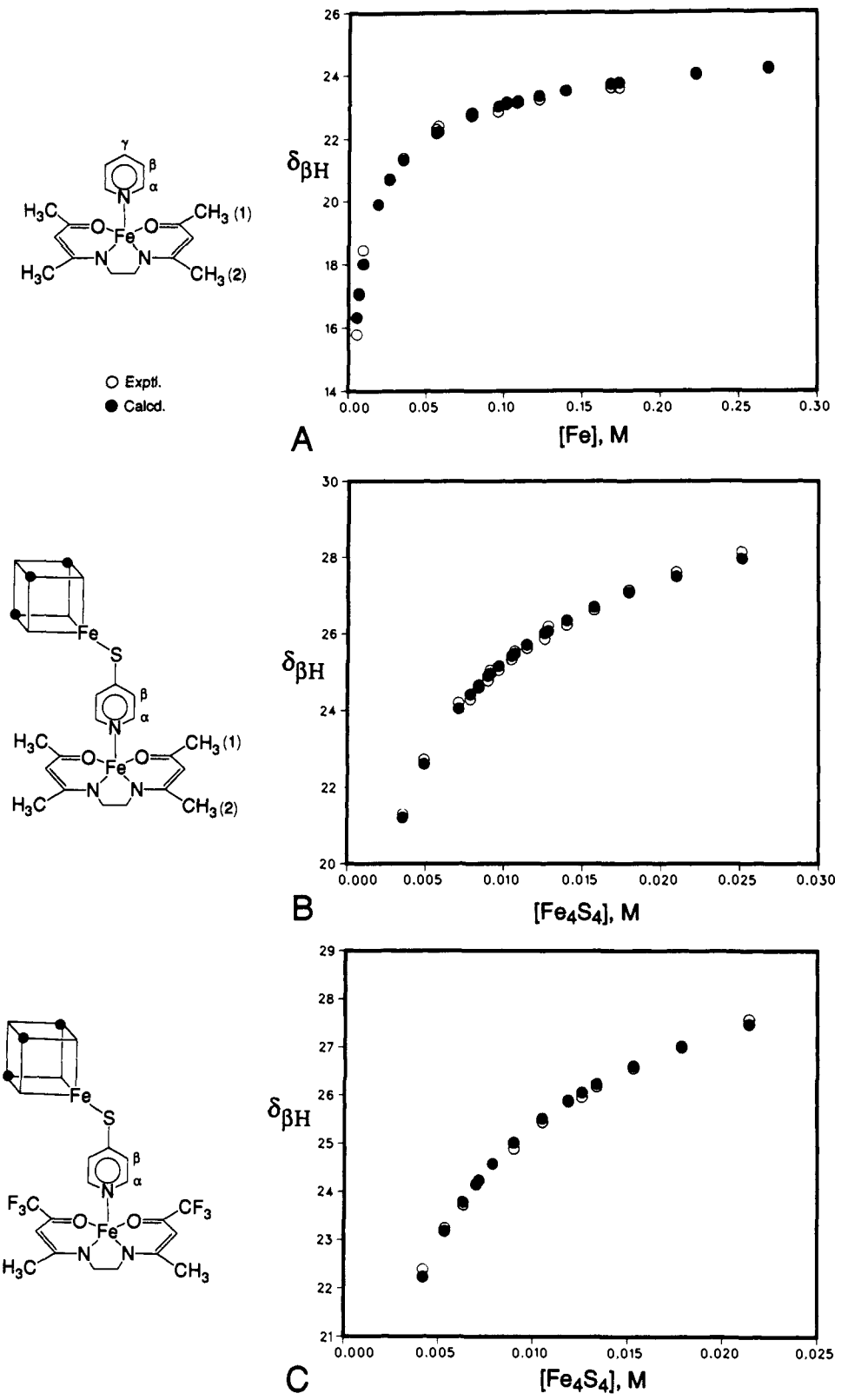

Figure 5. Comparison of the concentration dependence of the observed and calculated pyridine β-H chemical shifts in the equilibrium systems of reactions 9 (A), 7 (B), and 8 (C). The calculated points were evaluated by the method developed in the Appendix and utilizing the parameters in Table II.

bridge ligand that increases the negative charge at the nitrogen atom. Under the dilute concentration conditions of Figures 3C and 4C, the two bridged assemblies are formed to the extent of 80%. The excellent agreement between observed and calculated pyridine β-H chemical shifts based on these equilibrium constants and δ_1 values is demonstrated in Figures 5B and 5C.

The equilibrium constants for reactions 7–10 are comparable with those for unmodified and capped Fe(II) porphyrin complexes and for Fe(II)(phthalocyanine) listed in Table II. The much larger K_{f2} value for Fe(TPP)$(py)_2$ is associated with conversion to a low spin state upon binding a second pyridine. This effect is absent in Fe(tfacen)$(py)_2$, which remains high-spin.

Electron-Transfer Behavior. Relevant redox potentials are summarized in Table IV. In acetonitrile solution, Fe(acen) is irreversibly oxidized at E_{pa} = −0.09 V. Similar behavior was observed in dichloromethane solution at E_{pa} = +0.43 V (100 mV/s). However, in the presence of a stronger axial ligand, Fe(acen)(py) in acetonitrile undergoes a well-defined chemically

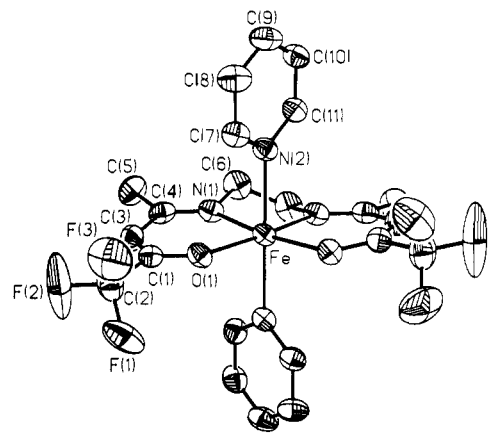

Figure 6. The structure of Fe(tfacen)$(py)_2$, showing 50% probability ellipsoids and the atom labeling scheme.

Table III. Selected Bond Distances (Å) and Angles (deg) for Fe(tfacenpy) and Fe(tfacen)$(py)_2$[a]

	Fe(tfacenpy)		
Fe–O(1)	1.983 (2)	O(1)–Fe–O(1′)	116.9 (1)
Fe–N(1)	2.168 (3)	O(1)–Fe–N(1)	96.5 (1)
Fe–N(2)	2.132 (2)	O(1)–Fe–N(2)	121.5 (1)
		N(1)–Fe–N(2)	84.3 (1)
		N(1)–Fe–N(1′)	168.6 (1)
N(1)–Fe–O(1′)/ N(1′)–Fe–O(1)	64.4		
N(1′)–Fe–O(1)/ C(8–10)N(2)	72.6		
	Fe(tfacen)$(py)_2$		
Fe–O(1)	2.024 (2)	O(1)–Fe–O(1′)	102.3 (1)
Fe–N(1)	2.115 (3)	O(1)–Fe–N(1)	88.4 (1)
Fe–N(2)	2.280 (3)	N(1)–Fe–N(1′)	81.1 (1)
		O(1)–Fe–N(2)	89.8 (1)
		N(2)–Fe–N(1)	90.7 (1)
		N(2)–Fe–O(1′)	87.2 (1)
		N(2)–Fe–N(1′)	93.0 (1)
		N(2)–Fe–N(2′)	175.2 (1)
O(1)–Fe–N(1)/ O(1′)–Fe–N(1′)	3.5		
C(7–11)N(2)/ C(7′–11)N(2′)	78.1		

[a] Primed and unprimed atoms are related by a C_2 axis.

reversible reaction ($i_{pc}/i_{pa} \approx 1$). The remaining reactions in Table IV are also chemically reversible. The effect of two trifluoromethyl groups on the Fe(II,III) potential is large, rendering Fe(tfacen)$(py)_2$ more difficult to oxidize than Fe(acen)(py) by 0.37 V. All clusters exhibit the standard 2−/3− redox reaction near −1 V. Inasmuch as positive potential shifts of the 2−/3− couple are found without exception when an alkylthiolate is substituted by an arylthiolate,[9,41] the observed difference of ca. 0.1 V between clusters **5**/**6** and **8**/**9** provides independent verification of ligand substitution. Potentials of the bridged assemblies are internally consistent with cluster and Fe(II) complex results. The Fe(II) site in **9**-Fe(acen) is more easily oxidized by 0.17 V than that in **9**-Fe(tfacen). These potentials are shifted to negative values compared to the monopyridine adducts. The electron-releasing tendency of the 4-thiolate substituent would be expected to enhance the stability of the Fe(III) state. Cluster potentials are not measurably affected by bridge formation. This is not an unexpected result inasmuch as in bridge formation only one cluster ligand is altered, at a point some distance from the cluster itself.

Summary

The following are the principal findings and conclusions of this investigation.

Table IV. Redox Potentials of Fe(II) Complexes, Clusters, and Bridged Assemblies

species	$E_{1/2}$,[a] V: $Fe^{III/II}$	$E_{1/2}$,[a] V: $[Fe_4S_4(LS_3)L']^{2-/3-}$
Fe(acen)	−0.09[b]	
Fe(acen)(py)	−0.21	
Fe(tfacen)(MeCN)	0.29	
Fe(tfacen)$(py)_2$	0.16	
Fe(tfacenpy)	0.26	
5		−1.06
6		−1.08
8		−0.97
9		−0.98
9-Fe(acen)	−0.37	−0.97
9-Fe(tfacen)	−0.20	−0.97

[a] Acetonitrile solutions, 297 K, vs SCE; concentrations (M × 10^3): Fe(II) complexes, 4.0–7.0; **5**–**9**, 1.5; **9**-Fe(acen), **9**-Fe(tfacen), 3.0. [b] Irreversible (E_{pa}) at 100 mV/s.

(1) Subsite-differentiated clusters **1** with L′ = alkylthiolate (**5** and **6**) undergo high yield ligand substitution reactions with pyridinethiols to afford clusters **8** and **9** with pyridyl nitrogen binding sites.

(2) Clusters **8** and **9** react with the complexes Fe(acen) and Fe(tfacen)(MeCN) to afford the bridged cluster assemblies **8**-Fe(acen), **9**-Fe(acen), and **9**-Fe(tfacen), whose formation can be recognized by changes in the isotropically shifted ^1H NMR spectra of the cluster, bridge, and Fe(II) complex portions of the assemblies. The latter retains the $S = 2$ ground state of the initial complexes.

(3) The systems Fe(acen)/py, Fe(tfacen)(MeCN)/py, and the bridged assemblies exist in equilibria involving bound and free Fe(II) complexes. Formation constants have been measured by an NMR method. Trifluoromethyl groups increase K_f values by 36% in the pyridine and 16% in the assembly systems; the 4-thiolate group enhances these values by a factor of ca. 2 in the bridged assembly reactions. In the assemblies, pyridyl-Fe(II) binding should structurally resemble that established for Fe(tfacen)$(py)_2$ but with a small displacement of the Fe(II) atom out of the O_2N_2 ligand plane in the direction of the bridge nitrogen atom.

(4) The change from irreversible to reversible oxidation of Fe(acen) in the presence of pyridine provides a second method of detecting axial ligation and assembly formation. Fe(II,III) potentials are rendered more positive by trifluoromethyl groups and more negative by the 4-thiolate substituent in bridged assemblies; cluster potentials are insensitive to assembly formation. The preparative and redox reactions generate the assembly oxidation levels $[Fe_4S_4]^{1+}$/Fe(II), $[Fe_4S_4]^{2+}$/Fe(II), and $[Fe_4S_4]^{2+}$/Fe(III). These are the three known oxidation levels of the active site of *Ec* SiR, but the synthetic assemblies do not necessarily contain the same cluster and Fe(II,III) spins as in the multiple oxidation and ligation states of the enzyme.

This work provides the initial experimental protocol for the construction of Fe_4S_4–Fe complex bridged assemblies. While bridged Fe_4S_4 clusters have been produced,[6,9,21] no other bridges from an Fe_4S_4 cluster to a dissimilar metal unit have been proven.[42] Experiments in progress are directed toward obtaining nonlabile assemblies based on clusters **8** and **9**. One solution to this problem involves the use of Fe complexes which become nonlabile (low-spin) upon binding to the pyridyl bridge and an exogeneous axial ligand (substrate). This would diminish lability of both bridge and axial ligand bonds. We have demonstrated the binding of Fe^{II}(OEP) to cluster **9**.

Another solution utilizes covalent attachment of the Fe complex to the bridge portion of the assembly, thereby eliminating bridge bond lability. The feasibility of this approach is sustained in part by the preparation of the quadridentate complex Fe(tfacenpy). Its structure is shown in Figure 7; selected molecular dimensions are included in Table III. There is an imposed 2-fold rotation

(41) DePamphilis, B. V.; Averill, B. A.; Herskovitz, T.; Que, L., Jr.; Holm, R. H. *J. Am. Chem. Soc.* **1974**, *96*, 4159.

(42) We note, however, the possibility of the mixed cluster assembly $Fe_4S_4/MoFe_3S_4$: Coucouvanis, D. *Acc. Chem. Res.* **1991**, *24*, 1.

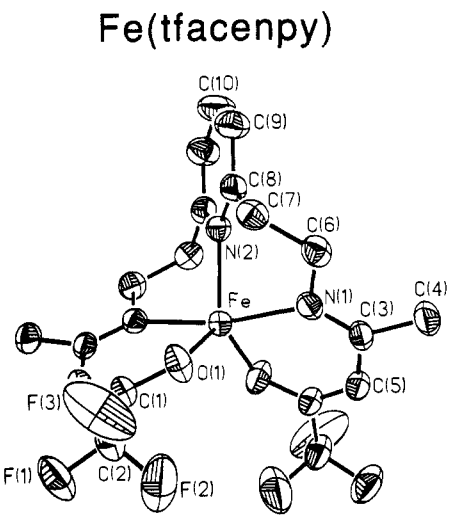

Figure 7. The structure of Fe(tfacenpy), showing 50% probability ellipsoids and the atom labeling scheme.

axis containing atoms Fe, N(2), and C(10). The coordination geometry is that of a distorted trigonal bipyramid, which has been set by ligand constraints, with the atoms O(1,1′)N(2) defining the equatorial plane. The contractile nature of the ligand is responsible for the relatively small difference (0.04 Å) in axial and equatorial bond lengths. In unconstrained Fe(tfacen)$(py)_2$, this difference is 0.16 Å. Fe(tfacenpy) undergoes a fully reversible oxidation at $E_{1/2}$ = 0.26 V. Thiol functionalization of the pyridine ring in this or other ligand systems derived from the parent diamine should permit the formation of a covalently bridged cluster assembly with a six-coordinate low-spin Fe(II) site. Research directed at the attainment of nonlabile assemblies is in progress.

Acknowledgment. This research was supported by NIH Grant GM 28856. X-ray equipment was obtained through NIH Grant 1 S10 RR 02247.

Appendix

Determination of Ligand Binding Constants by NMR. (a) Two Equilibria. The equilibrium constants for reactions 13 and 15 are given by eqs 14 and 16, respectively, where ML_n is some metal complex, Q is an additional ligand, and $c_0 = [ML_nQ_2]_0$.

$$ML_nQ_2 \rightleftharpoons ML_nQ + Q \quad (13)$$

$$K_1 = [ML_nQ][Q]/[ML_nQ_2] = x(x + 2y)/(c_0 - x - y) \quad (14)$$

$$ML_nQ \rightleftharpoons ML_n + Q \quad (15)$$

$$K_2 = [ML_n][Q]/[ML_nQ] = y(x + 2y)/x \quad (16)$$

Solving for y in eq 14

$$y = (K_1c_0 - K_1x - x^2)/(2x + K_1) \quad (17)$$

and substituting the result into eq 16 gives

$$(4K_2 - K_1)x^3 + (4K_1K_2 - K_1^2 + 2K_1c_0)x^2 + (K_1^2K_2 + 3K_1^2c_0)x - 2K_1^2c_0^2 = 0 \quad (18)$$

At fast exchange, the average chemical shift of a given nucleus in bound and free ligand is

$$\delta_{obs} = (2[ML_nQ_2]/2c_0)\delta_2 + ([ML_nQ]/2c_0)\delta_1 + ([Q]/2c_0)\delta_0 \quad (19)$$

where the subscripts refer to species with 2, 1, and 0 (free) Q ligands bound. All systems were monitored with the pyridine β-H resonance. In the Fe(tfacen)/py system, eq 19 was used, δ_0 = 7.32 ppm, $c_0 = [Fe(tfacen)(py)_2]_0$, and δ_1 and δ_2 were parameters.

(b) Single Equilibrium. The systems Fe(acen)/py, **9**/Fe(acen), and **9**/Fe(tfacen) were analyzed in terms of equilibrium 15, for which the equilibrium constant and the average chemical shift are given by

$$K_2 = x^2/(c_0 - x) \quad (20)$$

$$\delta_{obs} = ([ML_nQ]/c_0)\delta_1 + ([Q]/c_0)\delta_0 \quad (21)$$

For Fe(acen)/py, δ_0 = 7.32 ppm, $c_0 = [Fe(acen)(py)]_0$, and δ_1 is a parameter. For the other two systems, δ_0 = 5.89 ppm (from the spectrum of **9**), $c_0 = [\mathbf{9}]_0$, and δ_1 is a parameter.

The quantities K_2 and/or K_1 and δ_2 and/or δ_1 were determined by the Simplex algorithm in a sequential optimization method that involves repeated comparison between calculated and observed values. This procedure is a powerful technique for simulating parameters which best describe the behavior of data points. Accounts of the methods are available elsewhere.[43] As an example, for the system Fe(tfacen)/py, input data include known values of c_0 and δ_{obs} and estimated values of K_1,K_2 and δ_1,δ_2 and their step increments. The program calculates the roots of eq 18 by the Newton method, with the requirement that they make the lhs of eq 18 $< 1 \times 10^{-10}$. Of the three possible roots, the most physically meaningful is selected. The quantity y is then calculated from eq 17. With the values of x and y and the estimated values of δ_1 and δ_2, the shifts δ_{calc} are calculated from eq 19 for all data points (δ_{obs}) measured at different concentrations. These are then compared with δ_{obs} to establish consistency. If a match within a specified tolerance is not obtained, K_1,K_2 and δ_1,δ_2 are redetermined (x and y are recalculated) until agreement is reached. For the single equilibrium systems, an analogous procedure was followed using eqs 20 and 21. Finally, for the Fe(tfacen)/py system only the set of parameters K_1,K_2 and δ_1,δ_2 was accepted for which the δ_1 value was in good agreement with those of the other three systems, whose analysis required two parameters. The plots in Figure 5 demonstrate the satisfactory analysis of the data using this procedure. Values of the formation constants $K_{f1} = 1/K_2$, $K_{f2} = 1/K_1$ and δ_1,δ_2 are listed in Table II; note that the limiting values δ_1 occur in a relatively narrow range (8 ppm).

Registry No. $(Bu_4N)_2$[**5**], 137003-14-6; $\mathbf{5}^{3-}$, 137028-49-0; $(Bu_4N)_2$[**6**], 137003-15-7; $\mathbf{6}^{3-}$, 113088-02-1; $(Bu_4N)_2$[**7**], 137003-16-8; $(Bu_4N)_2$[**8**], 137050-96-5; $(Bu_4N)_2$[**8**-Fe(acen)], 137050-98-7; $\mathbf{8}^{3-}$, 137028-50-3; $(Bu_4N)_2$[**9**], 137028-45-6; $(Bu_4N)_2$[**9**-Fe(acen)], 137085-35-9; $(Bu_4N)_2$[**9**-Fe(tfacen)], 137028-48-9; $\mathbf{9}^{3-}$, 137050-99-8; [**9**-Fe(acen)]$^-$, 137003-24-8; [**9**-Fe(tfacen)]$^-$, 137028-51-4; [**9**-Fe(acen)]$^{3-}$, 137028-52-5; [**9**-Fe(tfacen)]$^{3-}$, 137056-96-3; $(Bu_4N)_2[Fe_4S_4(SMe)_4]$, 50923-26-7; $(Bu_4N)_2[Fe_4S_4(SEt)_4]$, 53433-48-0; H_2(tfacen), 433-30-7; H_2(tfacenpy), 137003-13-5; $FeCl_2$·1.5THF, 12562-70-8; [Fe(acen)], 108571-98-8; [Fe(acen)(py)], 108547-95-1; [Fe(tfacen)$(py)_2$], 137003-17-9; [Fe(tfacen)(MeCN)], 137003-18-0; [Fe(tfacenpy)], 137028-46-7; Na[Fe(acen)(SMe)], 137003-19-1; [Fe(acen)(py)]$^+$, 137003-20-4; [Fe(tfacen)(MeCN)]$^+$, 137003-21-5; [Fe(tfacen)$(py)_2$]$^+$, 137003-22-6; [Fe(tfacenpy)]$^+$, 137003-23-7; 1,1,1-trifluoropentane-2,4-dione, 367-57-7; ethylenediamine, 107-15-3; 2,6-bis(aminoethyl)pyridine, 60354-75-8.

Supplementary Material Available: Tables of X-ray crystallographic data for the compounds in Table I and tables of intensity collections, positional and thermal parameters, bond distances and angles, and calculated hydrogen atom positions (9 pages); table of calculated and observed structure factors (32 pages). Ordering information is given on any current masthead page.

(43) (a) Caceci, M. S.; Cadneris, W. P. *Byte* **1984**, 340. (b) Jurs, P. *Computer Software Applications in Chemistry*; John Wiley & Sons, Inc.: New York, 1986, Chapter 9.